Numerical Investigation of Solidification around a Circular Cylinder with the Presence of the Free Surface in a Rectangular Cavity

Nghiên cứu mô phỏng số quá trình hóa rắn xung quanh trụ tròn với sự hiện diện của mặt thoáng trong một khoang hình chữ nhật

Vu Van Truong*, Truong Viet Anh

Hanoi University of Science and Technology, No. 1, Dai Co Viet, Hai Ba Trung, Hanoi, Viet Nam

Received: June 06, 2016; accepted: December 20, 2016

Abstract

This paper presents numerical simulation of solidification around a cooled circular cylinder with the presence of a free surface in a rectangular cavity. The free surface is introduced to account for volume change due to density difference between the solid and liquid phases during solidification. Pure tin with the solid-to-liquid density ratio ρ_{sl} = 1.05 (shrinkage) is investigated as a phase change material. The front-tracking method combined with an interpolation technique, in which the interface separating two phases is represented by connected elements laid on a stationary grid, is used for solving the problem. The case of no volume change, i.e., ρ_{sl} = 1.0, is also calculated and compared with the case of ρ_{sl} = 1.05 to see how volume shrinkage affects the solidification process. The numerical results show that shrinkage reduces the solidification rate, and thus results in a decrease in the form, i.e., the area, of the solid layer around the cylinder. In addition, the liquid level decreases in time due to volume shrinkage upon solidification.

Keywords: Numerical simulation, Front-tracking, Solidification, Shrinkage, Circular cylinder

Tóm tắt

Bài báo giới thiệu mô phỏng số quá trình hóa rắn xảy ra xung quanh một trụ tròn được làm lạnh với sự hiện diện của mặt thoáng trong một khoang hình chữ nhật. Mặt thoáng được đưa vào để bù vào sự thay đổi về thể tích do sự khác nhau về khối lượng riêng giữa pha lỏng và pha rắn trong quá trình hóa rắn. Thiếc nguyên chất với tỉ số khối lượng riêng giữa pha rắn và pha lỏng ρ_{sl} = 1.05 (co thể tích) được nghiên cứu như là một vật liệu chuyển pha. Phương pháp theo dấu biên kết hợp với kỹ thuật nội suy mà ở đó biên phân cách giữa hai pha được biểu diễn bởi các đoạn thẳng liên kết, được sử dụng cho việc giải bài toán. Trường hợp không có sự thay đổi về tích với ρ_{sl} = 1.0 cũng được tính toán và so sánh với ρ_{sl} = 1.05 để thấy được ảnh hưởng của sự co thể tích đến quá trình hóa rắn. Kết quả mô phỏng cho thấy, sự co thể tích làm giảm tốc độ hóa rắn, và kéo theo giảm sự hình thành của miền rắn xung quanh trụ. Thêm vào đó, mực mặt thoáng giảm dần theo thời gian do sự co lại về thể thích trong quá trình hóa rắn.

Từ khóa: Mô phỏng số, Theo dấu biên, Hóa rắn, Co thể tích, Trụ tròn

1. Introduction

Solid–liquid phase change finds application in many systems and in nature including latent heat energy storage, metallurgy, and food and pharmaceutical processing. Solidification around cooled cylinders appears in thermal energy storage systems, metal casting and others. Therefore, understanding solidification heat transfer around cooled cylinders plays an important role in designing and operating such systems. Accordingly, there have been many works concerned with solidification around cylinders. Sasaguchi and co-workers [1] presented a numerical method for the solid–liquid phase change around a single cylinder and two horizontal cylinders in a rectangular cavity. A more complicated system in which there exist three or more cylinders has been investigated by Sugawara and Beer [2]. In another work [3], an enthalpy formulation-based fixed-grid approach was employed to investigate the solidification around a number of staggered cylinders. However, in the above-mentioned papers, the results were restricted to indentical densities of the solid and liquid phases. It has been reported that density differerence between the solid and liquid phases, which causes volume change upon solidification, may have strong effects on the final solidified products [4,5]. To account for this effect, it is neccessary to include a gas phase to the problem, i.e., there is the presence of the free surface. The investigations considering such above-mentioned aspects have not been reported in liturature.

* Corresponding author: Tel.: (+84) 915.058.146
Email: truong.vuvan1@hust.edu.vn

In the present study, we present numerical investigations for solidification around a cooled cylinder with natural convection and with the presence of the free surface. The method utilizes the front tracking technique [6] to represent the solid–liquid interface and an interpolation technique, i.e., an immersed boundary method, to deal with the no-slip and constant isothermal temperature boundary conditions [4]. Pure tin with the solid phase denser than the liquid phase, i.e., with volume shrinkage upon solidification, is used as an investigated phase change material.

2. Numerical problem and method

Fig. **1** shows the investigated problem, a solidification layer forming around a cooled circular cylinder held at temperature T_c with a free surface in a rectangular cavity. The diameter of the cylinder is denoted by d. The fusion temperature of the liquid (or melt) is T_m greater than T_c. Initially, the gas and liquid phases are at temperature T_0 ($T_0 \geq T_m$). To save the computations, the half of the physical domain is investigated as shown in

Fig. **1**a. The fluid and thermal properties of each phase are assumed constant, and the presence of the gas phase (i.e., free surface) is to account for volume change due to density difference between the solid and liquid phases during solidification. The fluids assumed incompressible are driven by buoyancy-induced natural convection, i.e., Bussinesq approximation. We treat all phases as one fluid with variable properties such as density ρ, viscosity μ, thermal conductivity k and heat capacity C_p. In terms of the one-fluid representation, the momentum and thermal energy equations are

$$\partial(\rho\mathbf{u})/\partial t + \nabla\cdot(\rho\mathbf{u}\mathbf{u}) = -\nabla p + \nabla\cdot\mu(\nabla\mathbf{u} + \nabla\mathbf{u}^T) + \rho\mathbf{f} + \int_f \sigma\kappa\mathbf{n}_f\delta(\mathbf{x}-\mathbf{x}_f)dS + \rho\mathbf{g}\beta(T-T_m) \quad (1)$$

$$\partial(\rho C_p T)/\partial t + \nabla\cdot(\rho C_p T\mathbf{u}) = \nabla\cdot(k\nabla T) + \int_f \dot{q}\delta(\mathbf{x}-\mathbf{x}_f)dS + \rho C_p h \quad (2)$$

$$\nabla\cdot\mathbf{u} = (1/\rho_s - 1/\rho_l)\int_f \delta(\mathbf{x}-\mathbf{x}_f)\dot{q}dS \Big/ L_h \quad (3)$$

Here, $\mathbf{u}$ is the velocity vector, p is the pressure, $\mathbf{g}$ is the gravitational acceleration, and t is time. T and the superscript T denote the temperature and the transpose. D/Dt is the material derivative. $\mathbf{f}$ is the momentum forcing term used to impose the no-slip condition on the solid–liquid interface, and h is the energy forcing term used to impose a constant temperature on the cylinder boundary [4]. The fourth term on the right-hand side of Eq. (1) accounts for the interfacial tension force at the free surface [7]. The last term in Eq. (1) is the Boussinesq approximation for density changes due to thermal gradients [8], and β is the thermal expansion coefficient of the fluids. At the interfaces, denoted by f, σ is the interfacial tension acting on the liquid–gas front. κ is twice the mean curvature, and $\mathbf{n}_f$ is the normal vector to the interface. The Dirac delta function $\delta(\mathbf{x} - \mathbf{x}_f)$ is zero everywhere except at the interfaces $\mathbf{x}_f$. $\dot{q}$ is the heat source at the solidification interface, given as

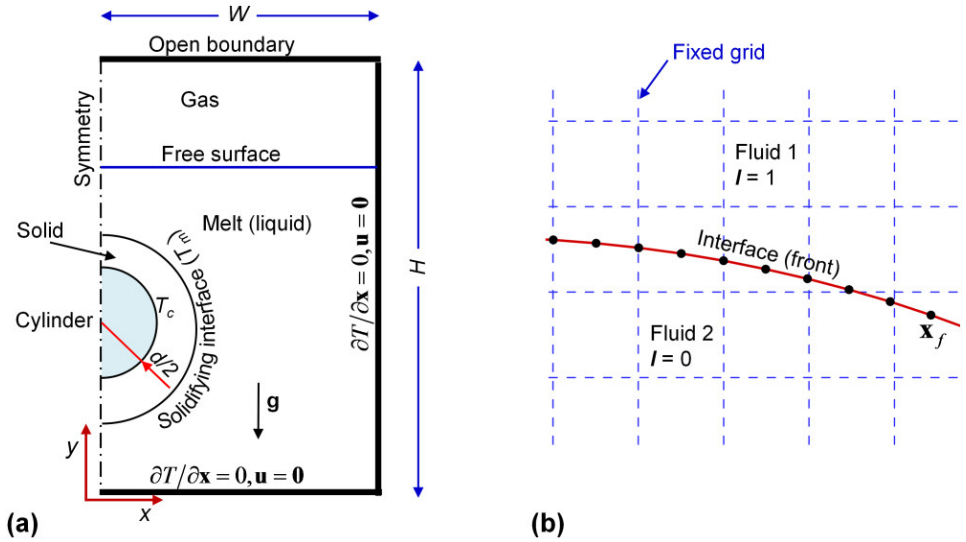

Fig. 1. Solidification around a cooled cylinder with the free surface in a rectangular cavity: (a) computational domain; and (b) front-tracking representation for the solidification and free surface interfaces.

$$\dot{q} = k_s \frac{\partial T}{\partial n}\bigg)_s - k_l \frac{\partial T}{\partial n}\bigg)_l = -\rho_s V_n L_h \quad (4)$$

where the subscripts s, l and g (when available) represent solid, liquid and gas, respectively. V_n is the velocity normal to the solidification front and L_h is the latent heat.

These above-mentioned equations are solved by the front-tracking method combined with interpolation techniques on a staggered grid with second order accuracy in time and space [4]. The momentum, energy and mass conservation equations are discretized using an explicit predictor-corrector time-integration method and a second-order centered difference approximation for the spatial derivatives. The discretized equations are solved on a fixed, staggered grid using the MAC method [9]. The interface between two phases is represented by finite discrete points, on a stationary grid as shown in Fig. **1**b, that are updated by

$$\mathbf{x}_f^{n+1} = \mathbf{x}_f^n + \mathbf{n}_f V \Delta t \quad (5)$$

where the superscripts n and n+1 are the current and next time levels. V is the velocity interpolated from the fixed velocity field for the points on the liquid–gas interface, and V_n for the points on the solidifying interface given by $V_n = -\dot{q}_f / (\rho_s L_h)$. Positions of the liquid–gas points are used to determine an indicator function I_l which is zero in the liquid and one in the gas, and positions of the solid–liquid points are used to determine an indicator function I_s which is zero in the solid and one in the liquid. The general equation for reconstructing $I_{s,l}$ is

$$\nabla I = \int_f \delta(\mathbf{x} - \mathbf{x}_f)\mathbf{n}_f dS \quad (6)$$

Accordingly, the values of the material property fields at every location are given as

$$\varphi = \varphi_g I_l + (1 - I_l)\left[\varphi_l I_s + (1 - I_s)\varphi_s\right] \quad (7)$$

where φ stands for ρ, μ, C_p, or k. A more detailed description of the method used in this study can be found in [4].

3. Numerical parameters

We choose the diameter d of the cylinder as a scaling length, and $\tau_c = \rho_l C_l d^2 / k_l$ as the characteristic time scale. The characteristic velocity scale is taken to be $U_c = d/\tau_c$. With these above choices, the dynamics of the problem is governed by the following dimensionless parameters: Prandtl number Pr, Stefan number St, Rayleigh number Ra, Weber number We, initial dimensionless temperature of the liquid θ_0, density ratios ρ_{sl} and ρ_{gl}, viscosity ratio μ_{gl}, thermal conductivity ratios k_{sl} and k_{gl}, heat capacity ratios C_{psl} and C_{pgl}, and expansion coefficient ratio β_{gl}:

$$Pr = \frac{C_{pl}\mu_l}{k_l}, St = \frac{C_{pl}(T_m - T_c)}{L_h}, Ra = \frac{g\beta_l (T_h - T_m) d^3 C_{pl} \rho_l^2}{\mu_l k_l},$$
$$We = \frac{\rho_l U_c^2 d}{\sigma}, \theta_0 = \frac{T_0 - T_c}{T_m - T_c}, \rho_{sl} = \frac{\rho_s}{\rho_l}, \rho_{gl} = \frac{\rho_g}{\rho_l},$$
$$\mu_{gl} = \frac{\mu_g}{\mu_l}, k_{sl} = \frac{k_s}{k_l}, k_{gl} = \frac{k_g}{k_l}, C_{psl} = \frac{C_{ps}}{C_{pl}}, \beta_{gl} = \frac{\rho_g \beta_g}{\rho_l \beta_l} \quad (8)$$

The temperature is non-dimensionalized as $\theta = (T - T_c)/(T_m - T_c)$. The dimensionless time is $\tau = t/\tau_c$.

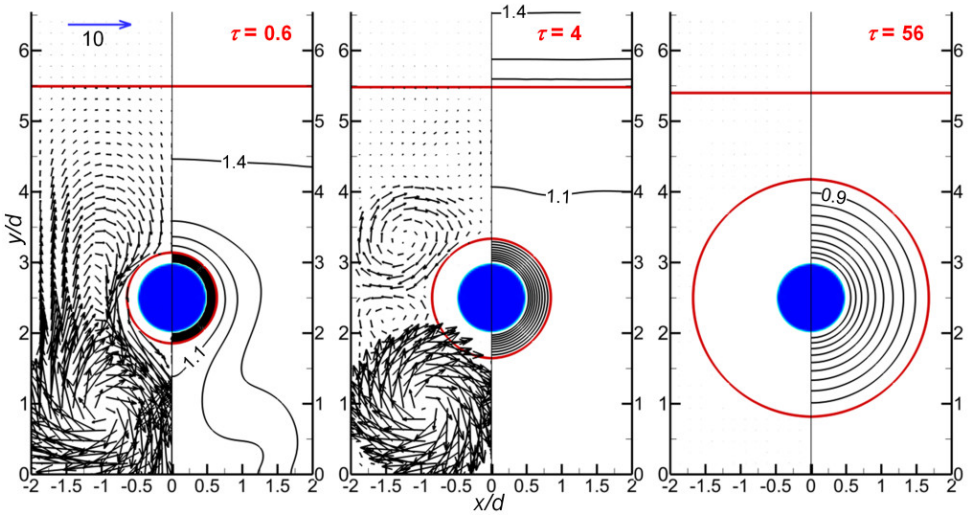

Fig. 2. Evolution of the solidification layer around the cooled cylinder with ρ_{sl} = 1.05. In each frame, the left shows the velocity field normalized by U_c, and the right shows the isotherms plotted every $\Delta\theta$ = 0.1

As previously mentioned, in this study, we focus only on the effects of volume change (ρ_{sl}) and thus other parameters are kept constant, i.e., Pr = 0.01, St = 0.02, Ra = 1×10^4, We = 5×10^{-4}, θ_0 = 1.42, ρ_{gl} = μ_{gl} = 0.05, k_{sl} = 1.0, k_{gl} = 0.005, C_{psl} = C_{pgl} = 1.0, and β_{gl} = 0.003. The values of these parameters correspond to pure tin with the cylinder diameter d of a few centimetres. The computational domain is $W\times H$ = $2d\times7d$ with a grid resolution of 64×224. The cylinder center is at x = 0, y = 2.5d, and the initial level of the liquid is 5.5d. Method validations have been extensively carried out in our previous works [4,7], and thus are not presented in this paper.

4. Results and discussion

Fig. 2 shows the temporal evolution of the solidifying and liquid–gas fronts with the temperature and velocity fields. The density ratio ρ_{sl} is set to 1.05. This density ratio is for tin. At early times of the solidification process, downward flow arises along the solid–liquid interface, at which the temperature is θ_m = 1.0, because the density of the liquid increases with a decrease in the temperature. As shown in the left frame (τ = 0.6) of Fig. 2, the downward flow is strong with the cooled liquid accumulating at the bottom part of the cavity. As a result, a thermally stratified region is formed. At later time τ = 4 (middle frame of Fig. 2), the flow decreases and three circulations with the strongest one at the bottom form. These circulations are induced by buoyancy, i.e., the last term in Eq. (1). As time progresses, the temperature of the liquid phase decreases to near the fusion temperature θ_m. Consequently, the flow is suppressed. At τ = 56 (right frame of Fig. 2), the liquid temperature is uniform in the entire cavity, and almost no flows are evident at this time, and the solidification process is merely controlled by conduction.

For tin, the solid is denser than the liquid, i.e., ρ_{sl} = 1.05, and this causes volume shrinkage during solidification. Accordingly, looking at the level of the liquid in the cavity, we can see that it decreases with time as shown in Fig. 2.

Fig. 3 shows the temporal variations of the average of the normal velocity of the solidifying interface, and of the space-averaged Nusselt number, at the sodifying interface, defined as

$$\overline{Nu} = \frac{1}{L_f}\int_0^{L_f}\left(\frac{\partial\theta}{\partial n}\right)_f dl \qquad (9)$$

where L_f is the length of the solidifying interface. During the initial stages of solidification, the temperature gradient at the solidifying interface is large, resulting in a high solidification rate, i.e., high $\overline{V_n}$, and high Nusselt number (Fig. 3). When the temperature in the liquid phase decreases and reaches the fusion temperature θ_m, the temperature gradient drops down, and $\overline{V_n}$ and $\overline{Nu}$ decrease (Fig. 3).

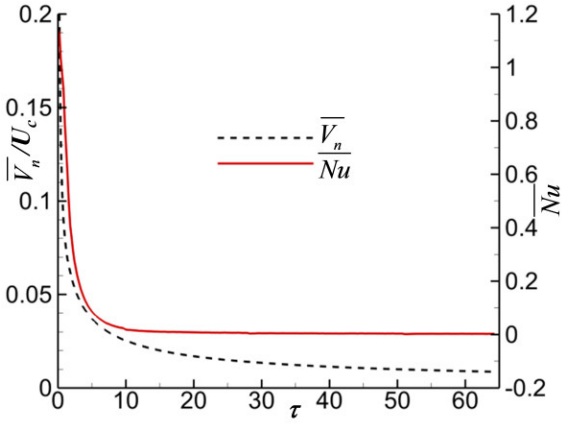

Fig. 3. Variations of the average solidifying velocity and of the space-average Nusselt number at the solidification interface with respect to time (ρ_{sl} = 1.05).

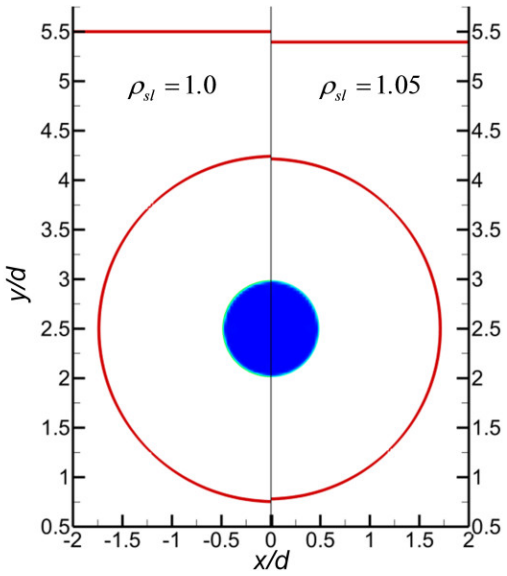

Fig. 4. Solidifying front and free surface location at τ = 60 for ρ_{sl} = 1.0 (left) and ρ_{sl} = 1.05 (right).

To consider how volume change affects the solidification process, we also perform simulation of a case with no density difference, i.e., ρ_{sl} = 1.0, and compare its results with those for ρ_{sl} = 1.05, as shown in

Fig. **4**. We can see that at this time as ρ_{sl} decreases from 1.05 to 1.0 the solid layer forming around the cylinder is wider. This indicates that the solidification rate decreases as ρ_{sl} increases. This is confirmed by Fig. 5, in which the area of the solid phase increases with a decrease in ρ_{sl} from 1.2 to 1.0 (one more case of ρ_{sl} = 1.2 has been calculated to show the effects of volume shrinkage). This is understandable since there is flow induced by density difference between the solid and liquid, coming to the solid layer to compensate [7,10] for ρ_{sl} = 1.05 and 1.2 (volume shrinkage). This flow reduces the solidification rate. Accordingly, the solid layer forming around the cylinder decreases for the case of shrinkage. In addition, as prevously mentioned, the level of the liquid phases decreases with time for the case of shrinkage while it does not change in the case of no volume change, i.e. staying at 5.5d, as shown in Fig. 5. Fig.5 also indicates that increasing this density ratio results in a faster decrease in the liquid level.

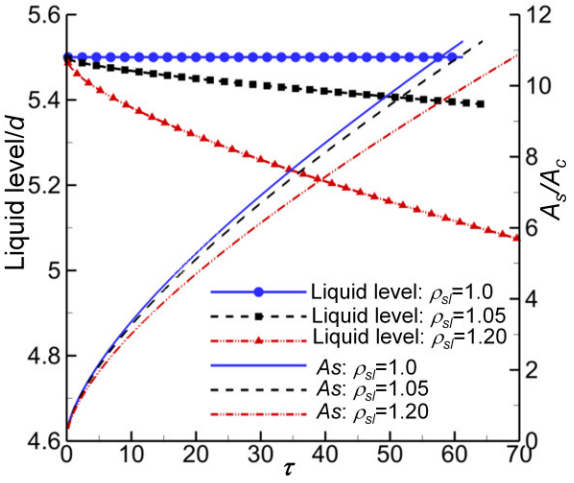

Fig. 5. Temporal variations of the level of the liquid phase and the area of the solid layer A_s around the cylinder for ρ_{sl} = 1.0, ρ_{sl} = 1.05, and ρ_{sl} = 1.2. A_c is the area of the cylinder.

5. Conclusion

We have presented the numerical results of solidification around a cooled cylinder in a cavity with the presence of volume shrinkage. To account for volume change during solidification, a gas phase was introduced at the top of the domain. Tin with ρ_{sl} = 1.05 was considered as a phase change material. The case of no volume change, i.e., ρ_{sl} = 1.0, was also calculated and compared with the case of volume change to demonstrate the effect of volume change on the solidication process. The front-tracking method combined with the interpolation technique [4] was used for solving the problem. The numerical results show that the presence of shrinkage reduces the solidication rate, and thus results in a decrease in the form, i.e., the area, of the solid layer around the cylinder. In addition, the liquid level decreases in time due to volume shrinkage. The results for ρ_{sl} = 1.2 are also presented.

Acknowledgments

This research is funded by Vietnam National Foundation for Science and Technology Development (NAFOSTED) under grant number 107.03-2014.21.

References

[1] K. Sasaguchi, K. Kusano, R. Viskanta, A numerical analysis of solid-liquid phase change heat transfer around a single and two horizontal, vertically spaced cylinders in a rectangular cavity, Int. J. Heat Mass Transfer. 40 (1997) 1343–1354.

[2] M. Sugawara, H. Beer, Numerical analysis for freezing/melting around vertically arranged four cylinders, Heat Mass Transfer. 45 (2009) 1223–1231.

[3] Y.-C. Shih, H. Chou, Numerical study of solidification around staggered cylinders in a fixed space, Numer. Heat Tr. A-Appl. 48 (2005) 239–260.

[4] T.V. Vu, A.V. Truong, N.T.B. Hoang, D.K. Tran, Numerical investigations of solidification around a circular cylinder under forced convection, J. Mech. Sci. Technol. 30 (2016) 5019–5028.

[5] S. Sablani, S.P. Venkateshan, V.M.K. Sastri, Numerical study of two-dimensional freezing in an annulus, J. Thermophys. Heat Tr. 4 (1990) 398–400.

[6] T.V. Vu, G. Tryggvason, S. Homma, J.C. Wells, H. Takakura, A front-tracking method for three-phase computations of solidification with volume change, J. Chem. Eng. Jpn. 46 (2013) 726–731.

[7] T.V. Vu, G. Tryggvason, S. Homma, J.C. Wells, Numerical investigations of drop solidification on a cold plate in the presence of volume change, Int. J. Multiphase Flow. 76 (2015) 73–85.

[8] H. Gan, J. Chang, J.J. Feng, H.H. Hu, Direct numerical simulation of the sedimentation of solid particles with thermal convection, J. Fluid Mech. 481 (2003) 385–411.

[9] F.H. Harlow, J.E. Welch, Numerical calculation of time-dependent viscous incompressible flow of fluid with free surface, Phys. Fluids. 8 (1965) 2182–2189.

[10] V.V. Truong, Direct numerical simulation of solidification with effects of density difference, Vietnam Journal of Mechanics. 38 (2016) 193–204.